Accuracy evaluation of RBC velocity measurement in nail-fold capillaries

Chih-Chieh Wu,[1] Wen-Chen Lin,[2] Geoffrey Zhang,[3] Chin-Wen Chang,[1] Ren-Shyan Liu,[4,5] Kang-Ping Lin,[2] Tzung-Chi Huang,[6,*]

[1]*Instrument Technology Research Center, National Applied Research Laboratories, Taiwan*
[2]*Department of Electrical Engineering, Chung Yuan Christian University, Taiwan*
[3]*Department of Radiation Oncology, Moffitt Cancer Center, Florida, USA*
[4]*Department of Nuclear Medicine, Taipei Veterans General Hospital, Taiwan*
5*Department of Nuclear Medicine, Medical School, National Yang-Ming University, Taiwan*
[6]*Department of Biomedical Imaging and Radiological Science, China Medical University, Taiwan*
[*]*Corresponding author: tzungchi.huang@mail.cmu.edu.tw*

Abstract: Cutaneous red blood cell velocity in vivo can be measured by using capillaroscopy with image processing techniques. However, unlike simulated blood flow images, there is no standard to determine the accuracy of the techniques for computing blood flow velocities. In this paper, we quantitatively evaluated the accuracy of previously proposed optical flow method for measuring red blood cell velocity in nail-fold capillaries. Blood flow images of subjects under normal and occlusion-release conditions were examined by a capillaroscope. To obtain velocity values, the images were further analyzed by using optical flow, cross-correlation and visual inspection methods, respectively. Visual inspection method was taken as the golden standard to determine the accuracy of blood flow velocity measurement using optical flow and cross-correlation techniques. Results showed that optical flow estimation provided superior accuracy to cross-correlation when assessing real blood flow velocity in nail-fold capillaries. Optical flow estimation is able to measure red blood cell velocity with a high accuracy of 91% and 86% when the observed velocity is less than 0.5 mm/s under normal and occlusion-release conditions, respectively. In addition, optical flow method showed good agreement with visual inspection in determining blood flow velocity in both normal and occlusion-release conditions when the high-velocity zone is excluded.

Keywords: red blood cell velocity, optical flow, cross-correlation, visual inspection

1. Introduction

Cutaneous red blood cell (RBC) velocity in capillaries is an important parameter in clinical hemorheology and microcirculation. The change of RBC velocity is a quantity which is frequently assessed under different biological and/or pathophysiological conditions. In an experimental study, Richardson et al. (1985) analyzed the ischemia effect on blood flow velocity in nail-fold of human toes. In a clinical study, Chang et al. (1996) investigated the clinical correlation of cutaneous microcirculation in patients with tetralogy of Fallot. The same research group also reported the relationship between cutaneous microcirculation and retinopathy in diabetes mellitus (Chang et al., 1997). There are several methods developed for the measurement of RBC velocity. To the best of our knowledge, several pioneer works for measuring RBC velocity were proposed since 1960s by Branemark and Jonsson (1963), Asano et al. (1964) and Muller (1966). Wayland and Johnson (1967) proposed the dual slit photometric technique which used two photodetectors separately located at the center line of a vessel, projected images onto a screen and recorded the time delay of intensity signals produced from the blood flow to determine RBC velocity. Intaglietta et al. (1970) developed a cross-correlation (C-C) method and applied it on a television system to measure the RBC velocity on-line. During the period of 1977 to 1990, cross-correlation technique had been

continuously modified and improved for the determination of RBC velocity (Fagrell et al., 1977; Intaglietta and Tompkins, 1987; Intaglietta et al., 1990). Recently, a few approaches have shown that it is possible to extract quantitative information from the microcirculatory images. For example, a digital microcirculatory image (DMCI) workstation (Ying and Xiu, 1994) and a real-time monitoring system were based on dual slit methodology (Sapuppo et al., 2004). Space-time diagram and line shift diagram were based on similar frame-to-frame examination to determine RBC velocity (Ellis et al., 1992; Klyscz et al., 1997; Japee et al., 2005; Dobbe et al., 2008). All these works reported that the RBC velocity is an important factor related to several diseases and represented the several methods for blood flow velocity estimation. However, the accuracy in RBC velocity estimation was still lacked.

In a previous study, we developed an automatic RBC velocity estimation system that enables optical flow method (OFM) based measurement of RBC velocity in a complete, clip-shape capillary (Wu et al., 2009). In another study, we discussed the use of three techniques in RBC velocity measurement with simulated blood flow images (Huang et al., 2010). OFM, space-time diagram (Hough transform based estimation) and cross-correlation method (CCM) are feasible and common solutions for RBC velocity determination. Among those three approaches, OFM demonstrates the highest accuracy in RBC velocity calculation with simulated blood flow patterns of micro-vessels. However, real blood flow images in nail-fold capillaries are usually noisy and the image quality is further affected by the limitation of capillaroscopy and/or finger jiggling artifact that was magnified by the microscope during observation. In this study, to evaluate the accuracy of the OFM approach with real human microcirculation images, visual inspection (VI) method was taken as a reference.

Blood flow videos were obtained from two groups of healthy volunteers. First, ten vessels from four healthy volunteers at rest condition were examined. Second, twelve vessels from another three healthy volunteers were assessed. The blood flow was controlled over a time period under four occlusion-release conditions which was performed by pumping a cuff wore on the subject's wrist. The RBC velocity varied correspondingly to the pressure conditions. Velocity data obtained at the arteriolar site, curve and venular site were examined by OFM, CCM and VI techniques for evaluation and comparison.

2. Materials and methods

2.1 Image acquisition

The capillaroscopy device, M320 (JMC Corporation, Kyoto, Japan), is a peripheral nail-fold capillary observation unit that consists of an objective lens, a charge coupled device (CCD) camera, a liquid crystal display (LCD) monitor, and four white light emitting diodes (LEDs). Video recorder acquired real-time blood flow video at a ×380 magnification, with a spatial resolution of 1.42 μm and image sampling rate of 30 frames per second (fps). The static image pixel matrix size was 720×480 and the field of view was 1×0.68 mm^2. Video signals were digitized by a computer via an image capture board and record onto a hard drive as DV-AVI files.

2.2 Visual inspection method for RBC velocity calculation

The principle of the frame-to-frame VI method is to determine the blood velocity by directly observing the movement of cells or plasma gaps between two consecutive frames. Usually, the frame-to-frame VI method is not considered as an efficient solution for measuring RBC velocity because it is time consuming and user interactive. Automatic analysis using this method can hardly be achieved. Nevertheless, if the image contrast is improved after image pre-processing, the frame-to-frame VI method can be applied to determine RBC velocity accurately. One consideration of the frame-to-frame VI is that the judgment of RBC movement between two frames is subjective to observers. So, we visually measured the velocity from the slopes of stripes on the space-time diagram (V_{std}) and averaged it with the result of the frame-to-frame method (V_{f2f}) to obtain the reference velocity (V_{ref}). Therefore, the combination of two VI results was used as the standard to evaluate and compare CCM and

OFM techniques. To generate a space-time diagram, the analyzed vessel on all of the consecutive frames was registered to the same position first. The gray-scale intensity of the center line of vessel from each positioned frame was extracted and sequenced to form horizontal lines in the space-time diagram (see Wu et al., 2009 for details of the center line extraction algorithm). All frames (lines) were put next to each other in vertical direction along the vertical time axis. When cells travel through the vessel, stripes are formed on the space-time diagram. The velocities of cells were determined from the slopes of stripes on the diagram. Fig. 1(a) illustrates three consecutive frames where plasma gap movement was observed. With the frame-to-frame VI, the plasma gap in the venous site was chosen and regarded as a buoy floating in the blood flow. The red square in the image indicates the position of the plasma gap. The movement of the plasma gap was quantified by the Euclidean distance between the red squares in two consecutive frames. The Euclidean distance was calculated based on the coordinates of two pixels in adjacent images. The coordinates were derived from the centroids of the plasma gaps or cells in the frames. A simulated space-time diagram generated from the three consecutive frames is shown in Fig. 1(b). Imagine that the plasma gap traveled through the vessel that depicted a track (the white stripe) in the diagram. V_{std} was obtained by calculating the slope of the stripe. The reference RBC velocity, V_{ref}, which was derived from the average of V_{f2f} and V_{std} was considered as the standard for evaluation and comparison studies.

2.3 RBC velocity calculation under normal flow condition

Ten 10-s videos of nail-fold micro-vessels were acquired from four healthy individuals while the subjects were in resting condition. The selection of velocity assessment was based on whether the frames generate clear stripes on the space-time diagram. Velocity values were determined for 25 sampling time points, with each point using at least 6 frames per assessment.

One of the analyzed vessels and its space-time diagram is shown in Fig. 2. Seven red stripes on the space-time diagram indicate that seven averaged velocity can be obtained from these groups of sampling frames. We selected about equal numbers of velocity assessment points from arteriolar, curve and venous sites of the 10 vessels. The mean and standard deviation of the length of the 10 vessels is 284±46.9 μm.

For RBC velocity estimation based on CCM (V_{CCM}), we used 1-window cross-correlation with a 30-pixel viewing window and a 40-pixel searching distance. Pixel intensity was averaged over the neighbor pixels within a 7-pixel wide square which is similar to the physical size of a RBC. According to the maximal correlation coefficient, the delays of pixel at the observed position were averaged over at least 6 frames. The OFM computation calculated two velocity vectors (Vx and Vy) at the observed point $p(x,y)$ from two consecutive images. The velocity (V_{OFM}) at p is determined using Eq. (1),

$$V_{OFM} = \sqrt{V_x^{\,2} + V_y^{\,2}} \qquad (1)$$

2.4 RBC velocity calculation with occlusion-release flow condition

For the purpose of simulating different blood flow velocity patterns in capillaries, an occlusion-release experiment was performed in which the protocol described in our previous study (Wu et al., 2009) was followed. A cuff was applied on the volunteer's wrist and its pressure was controlled by an in-house made electronic pump controller throughout a 45-second acquisition. Twelve vessels were selected from images of three subjects. The blood flow videos were recorded for four flow phases: resting (T_1), inflation (T_2), occlusion (T_3) and release (T_4) (see Fig. 3).

The cuff pressure was set at zero in T_1 and the blood flow video was recorded for 10 seconds. Then, the pressure linearly increased from zero to 180 mmHg in T_2 within 15 seconds. In T_3, the cuff pressure was fixed at 180 mmHg for 10 seconds. In the last phase, T_4, the pressure was released and dropped to zero in a few seconds. For each 45-second video, a

few time points from each condition were assessed for velocity computation. Again, sampling points were selected if the frames make clear stripes on the space-time diagram. For each point, the reference velocity was calculated and averaged from at least six consecutive frames. A total of 50 data points out of 12 vessels were calculated. One of the vessels and its space-time diagrams from T_1 to T_4 were shown in Fig. 4 as an example. Red stripes in the diagrams indicate the sampling frames. The blood flow in T_1 is under normal condition. The majority of the frames in the inflation phase, T_2, showed a normal flow similar to those in T_1. As the pressure increased to 180 mmHg, slower flow was observed in the last few frames in T_2. In the occlusion phase, T_3, the flow was stopped and flow reversals occurred due to vessel occlusion. In the release phase, T_4, blood flow rose to peak and then recovered to normal at resting condition. About equal numbers of velocity assessment points in arteriolar, curve and venous sections of each vessel were selected. The mean and one standard deviation of length of the 12 vessels is 295.6±23.8μm. We applied CCM and OFM to measure RBC velocity with the capillary videos of various pressure phases.

3. Results

3.1 Error rate evaluation—normal flow condition

The velocity error (V_{err}) is the difference between V_{CCM} and V_{ref}, and between V_{OFM} and V_{ref}. The relative errors, which are the ratios of V_{err} to V_{ref}, in CCM and OFM estimations, are illustrated in Fig. 5. The mean relative error of velocity and one standard deviation for 1-window CCM and OFM against V_{ref} are 25.97±21.39% and 11.43±10.25% respectively. Absolute values were applied on the calculation of mean relative error and one standard deviation of velocity while the original values were shown in Fig. 5.

3.2 Error rate evaluation—occlusion-release flow condition

In resting condition, T_1, observed values (16 data for each method) of RBC velocity were lower than 350 μm/s. Blood flow was not affected by the wrist cuff in T_1. The mean relative error of velocity and standard deviation of CCM and OFM measurements were 22.72±20.72% and 7.70±8.95% respectively (see Fig. 6(a)). In the inflation phase, T_2, observed values (11 data for each method) of RBC velocity were lower than 250 μm/s. The blood flow pattern in T_1 and T_2 was similar except for the deceleration in the last few seconds in T_2. The mean relative error of velocity and one standard deviation were 11.72±8.19% (CCM) and 12.35±8.38% (OFM) respectively (see Fig. 6(b)). In the occlusion phase, T_3, observed values (11 data for each method) of RBC velocity were lower than 60 μm/s. Blood flow was almost stopped as the cuff pressure kept at 180 mmHg during the entire phase. Small magnitude of back-and-forth movements of RBCs was observed occasionally. The mean error rate and its standard deviation of CCM and OFM were 32.59±16.28% and 28.25±27.14% respectively (see Fig. 6(c)). In the release phase, T_4, observed values (12 data for each method) of RBC velocity were lower than 830 μm/s. The cuff pressure was released to 0 mmHg. The blood flow increased to the peak and then returned to resting condition. The mean relative error and standard deviation of velocity that evaluating by CCM and OFM were 26.52±13.99% and 19.29±24.52% respectively (see Fig. 6(d)).

The relative errors of the velocity estimations using CCM and OFM for the entire acquisition (T_1 to T_4) were shown in Fig. 7(a) where 50 data points were presented. The mean relative error and one standard deviation of velocity of CCM and OFM were 23.38±17.18% and 16.03±19.65% respectively. The OFM velocity estimations usually gave lower values than the reference valuse especially when the velocity was higher than 200 μm/s. Errors by OFM usually were higher with higher velocities. If exclude the three highest values that are greater than 500 μm/s, the accuracy of OFM would be improved to 86%.

The data collected in normal condition were combined with the data from the occlusion-release study. A total of 75 data was illustrated in Fig. 7(b). The mean relative error and one standard deviation of CCM and OFM were 24.25±18.59% and 14.50±17.16% respectively. The tendency of higher error in high-velocity values remained.

3.3 Comparison—normal flow condition

To compare a new method of measurement with a standard method, Bland and Altman (1986; 1995) proposed a plot of the difference against the average of the new and standard measurements. The graphical technique, Bland—Altman plot, is more appropriate to statistically assess agreement between two methods than the use of correlation coefficients (*r*). The comparisons of CCM against VI and OFM against VI were performed by applying Bland—Altman plots in this study.

The agreement between CCM and VI for RBC velocity estimation is shown in a Bland—Altman plot (Fig. 8(a)). The mean difference is close to zero (-0.033 mm/s). There are 92% of values located in the limits of agreement. The agreement between the OFM estimation and VI is shown in Fig. 8(b). The mean difference of is almost zero (-0.04 mm/s). Greater differences are found at high velocity values. About 92% of the values are within the limits of agreement. For OFM against VI, the differences are small when the velocity is less than 0.5 mm/s which is consistent with the relative errors shown in Fig. 5. If the three highest data that are greater than 0.5 mm/s were excluded, the Bland and Altman plot yields a good agreement between OFM and VI estimations of normal RBC velocity.

3.4 Comparison—occlusion-release flow condition

The agreement between CCM and VI for RBC velocity measurement in four various flow conditions (T_1 to T_4) is shown in Fig. 9(a) through 9(d). For T_1, T_2, T_3 and T_4, values that fall within the limits of agreement were 94%, 91%, 91% and 92% respectively. For the entire acquisition (T_1 to T_4, see Fig. 9(e)), the mean difference is -0.014 mm/s.

For the four various conditions, the agreement of OFM and VI is shown in Fig. 10(a) through 10(d). For T_1, T_2, T_3 and T_4, values that are within the limits of agreement were 94%, 100%, 91% and 92% respectively. For the entire acquisition (T_1 to T_4), the mean difference is -0.03 mm/s (Fig. 10(e)). With the exclusion of the two highest difference values that are greater than 0.4 mm/s, good agreement between OFM and VI for RBC velocity calculation can be observed in Fig. 10(e). The standard deviation range on the Bland—Altman plots of T_2 and T_3 for both CCM and OFM was smaller than that of T_1 and T_4. It implies a relatively small variation of RBC dynamics during the vessel occlusion, which is consistent with the observations by Mathura et al. (2001) and Rosen et al. (1990).

The combination of data in normal and various flow conditions were analyzed to compare the agreement between CCM and VI, OFM and VI by Bland—Altman plots (Fig. 11 (a) and (b)) respectively. For CCM and OFM, 94.6% and 96% of values were within the limits of agreement respectively. In reference to the VI measurement, OFM shows better agreement for RBC velocity estimation in both normal and occlusion-release vessels if the high-velocity zone is excluded.

The mean differences and limits of agreement of RBC velocity in the Bland—Altman plots are summarized in Table 1.

4. Discussion

Laser Doppler flowmetry is frequently used to measure blood flow of vessels in vivo. Although it is able to quantify blood flow of capillaries, its resolution is not as high as the capillaroscopy that is able to assess blood flow dynamics in one single microvascular with a diameter similar to the size of the RBC (typically several micrometers). Therefore, we evaluated the accuracy of OFM and CCM for RBC velocity measurement by comparing them to VI estimation. The idea of combing the frame-to-frame and space-time diagram methods as a standard is because these two methods are intrinsically based on the same theory to calculate RBC velocity from the movement of plasma gap between consecutive frames. Space-time diagram method can be considered as an averaged frame-to-frame visual inspection method. Therefore, we combined the two methods to provide local and global (averaged) movements of plasma gap.

The first evaluation experiment was focused on the subjects in normal blood flow condition. OFM provided superior velocity accuracy to CCM when assessing real blood flow in nail-fold capillaries. The error distribution of CCM was scattered with larger errors at lower velocity values. Since the view window size was 30 pixels, it might not be sensitive enough to detect true local variations of velocity. Therefore, large errors were occasionally found at low velocities. Most of the velocities were underestimated when the value was above 200 μm/s for both CCM and OFM. They tend to give lower velocity values than the reference. For the OFM, relatively large errors were presented in the high velocity zone. With the exclusion of the three highest points that are greater than 500 μm/s, the accuracy of OFM is improved up to 91%. The significant high-velocity errors should be resulted from the violation of the constant brightness and velocity smoothness assumptions for OFM computation. If the contents of the vessel (RBCs and plasma gaps) move so fast in one frame, part of the contents might sneak out of the end of venous and disappeared in the next frame. In this case, the assumption of brightness conservation is violated which decreases the accuracy of OFM.

In the second evaluation experiment, four different blood flow conditions were set to evaluate the accuracy of OFM and CCM. In resting condition, T_1, the accuracy of OFM was 92% which was similar to that in normal flow condition if high-velocity values are excluded. Only one considerable error occurred when the velocity was higher than 300μm/s. In contrast, the accuracy of CCM is relatively poor at low velocities, say, less than 100 μm/s. Again, this might be resulted from the insensitivity to local variation by using the relatively large viewing window. In the inflation phase, T_2, the accuracy values of CCM and OFM were slightly lower than 90%. For both methods in T_2, the errors did not demonstrate a tendency in respect to velocity values. In the occlusion phase, T_3, the accuracy values of CCM and OFM are both around 70%. When the velocity is close to 1 pixel per frame, large percentage of errors might happen. In this case, even if a half-pixel difference will result in a 50% error. This kind of errors dominated the errors of the velocity measurement in this phase since the movement of RBCs was almost zero. In the release phase, T_4, The accuracy value of OFM was around 80%. Two instant peaks of velocity higher than 600 μm/s contributed large errors. Otherwise, the accuracy is as good as that in T_1 for OFM.

The parameters involved in CCM estimation such as the viewing window size and searching distance will influence the error in the RBC velocity estimation. In general, a smaller-size viewing window is appropriate to present local variation of blood flow but it is more sensitive to noise than a large window. The searching distance determines the maximum RBC velocity that can be measured by using CCM. In our study, a 40-pixel searching distance means that the maximum available RBC velocity is about 1700 μm/s. Using space-time diagram to calculate RBC velocity, the slopes can be measured visually or computed by automatic Hough transform technique (Dobbe et al., 2008). The maximal available velocity is determined from the vessel length (L, μm) and frame rate (F) of the camera. The same plasma gap should exist in at least three consecutive frames to present a reliable stripe. Therefore, the maximal available RBC velocity using space-time diagram method is LF/3 (μm/sec) (Dobbe et al., 2008). When we examined the arteriolar site or the venous site, the half- length of vessel approximates to 200 μm which results in a maximal available velocity of 2000 μm/s. For the curved part of vessel, the length L and corresponding maximal available velocity are decreased.

5. Conclusion

This study evaluates the accuracy of optical flow and cross-correlation methods for RBC velocity estimation in nail-fold capillaries. Blood flow videos were obtained from two groups of volunteers that were under normal and occlusion-release conditions respectively. Visual inspection was also applied to estimate the RBC velocity which was taken as a reference for the evaluation and comparison. OFM presented higher accuracy than CCM in RBC velocity estimation in normal (91%) and occluding-releasing blood flow conditions (86%). The good agreement of optical flow and visual inspection methods was reflected in the Bland—Altman plot, which indicates these two approaches are equivalent when applied in clinics.

In future work, in order to improve the accuracy of optical flow estimation in the high-velocity field, multi-resolution smoothing pre-processing technique may be performed for large motion estimation using optical flow (Sarker and Bechkoum, 2006). In addition, a high-speed camera will increase the frame rate and shorten the RBC movement between two consecutive frames which make it more accurate to estimate RBC velocity by using optical flow technique.

References

1. Asano, M., Yoshida, K., Tatai, K., 1964. Blood flow rate in the microcirculation as measured by photoelectric microscopy. Bull. Inst. Publ. Health 13, 201-204.
2. Bland, J. M., Altman, D. G., 1986. Statistical methods for assessing agreement between two methods of clinical measurement. Lancet i, 307-310.
3. Bland, J. M., Altman, D. G., 1995. Comparing methods of measurement why plotting difference against standard method is misleading. Lancet 346, 1085-1087.
4. Branemark, P.I., Jonsson, I., 1963. Determination of the velocity of corpuscles in blood Capillaries. A flying spot device. Biorheology 1, 143-146.
5. Chang, C.-H., Yu, H.-S., Chen, G.-S., Wu, J.-R., Huang, T.-Y., Yu, C.-L., 1996. Deterioration of cutaneous microcirculatory status and its clinical correlation in tetralogy of Fallot. Microvasc. Res. 51, 59-68.
6. Chang, C.-H., Tsai, R.-K., Wu, W.-C., Kuo, S.-L., Yu, H.-S., 1997. Use of Dynamic Capillaroscopy for Studying Cutaneous Microcirculation in Patients with Diabetes Mellitus. Microvasc. Res. 53, 121-127.
7. Dobbe, J. G. G., Streekstra, G. J., Atasever, B., Zijderveld, R. van, Ince, C., 2008. Measurement of functional microcirculatory geometry and velocity distributions using automated image analysis. Med. Biol. Eng. Comput. 46, 659–670.
8. Ellis, C.G., Ellsworth, M.L., Pittman, R.N., Burgess, W.L., 1992. Application of image analysis for evaluation of red blood cell dynamics in capillaries. Microvasc. Res. 44, 214–225.
9. Fagrell, B., Fronek, A., Intaglietta, M., 1977. A microscope-television system for studying flow velocity in human skin capillaries. Am. J. Physiol. Heart Circ. Physiol. 233, H318-H321.
10. Huang, T.-C., Lin, W.-C., Wu, C.-C., Zhang, G., Lin, K.-P., 2010. Experimental estimation of blood flow velocity through simulation of intravital microscopic imaging in micro-vessels by different image processing methods. Microvasc. Res. 80, 477–483.
11. Intaglietta, M., Tompkins, W. R., Richardson, D. R., 1970. Velocity measurements in the microvasculature of the cat omentum by on-line method. Microvasc. Res. 2, 462-473.
12. Intaglietta, M., Tompkins, W. R., 1987. Capillary video red blood cell velocimetry by cross-correlation and spatial filtering. Microvasc. Res. 34, 108-115.
13. Intaglietta, M., Breit, G. A., Tompkins, W. R., 1990. Four window differential capillary velocimetry. Microvasc. Res. 40, 46-54.
14. Japee, S.A., Pittman, R.N., Ellis, C.G., 2005. A new video image analysis system to study red blood cell dynamics and oxygenation in capillary networks. Microcirculation 12, 489-506.
15. Klyscz, T., Jünger, M., Jung, F., Zeintl, H., 1997. Cap image – a new kind of computer-assisted video image analysis system for dynamic capillary microscopy. (in German) Biomed. Tech. (Berl) 42, 168–175.
16. Mathura, K.R., Vollebregt, K.C., Boer, K., Graaff, J.C. De, Ubbink, D.T., Ince, C., 2001. Comparison of OPS imaging and conventional capillary microscopy to study the human microcirculation. J. Appl. Physiol. 91, 74-78.
17. Muller, H., 1966. Erythrocyte transit time technique. Methods Med. Res. 11, 207-211.
18. Richardson, D., Schwartz, R., Hyde, G., 1985. Effects of ischemia on capillary density and flow velocity in nailfolds of human toes. Microvasc. Res. 30, 80-87.
19. Rosen, L., Ostergren, J., Fagrell, B., Stranden, E., 1990. Mechanisms for edema formation in normal pregnancy and preeclampsia evaluated by skin capillary dynamics. Int. J. Microcirc. Clin. Exp. 9, 257-266.
20. Sapuppo, F., Longo, D., Bucolo, M., Intaglietta, M., Arena, P., Fortuna, L., 2004. Real time blood flow velocity monitoring in the microcirculation. Conf. Proc. IEEE Eng. Med. Biol. Soc., 2219-2222.
21. Sarker, M.H., Bechkoum K., 2006. Gradient-based optical flow for large motion using multi-resolution smoothing operation pre-processing technique. Malayas. J. Comput. Sci. 19, 141-149.
22. Wayland, H., Johnson, P.C., 1967. Erythrocyte velocity measurement in microvessels by a two-slit photometric method. J. Appl. Physiol. 22, 333–337.
23. Wu, C.-C., Zhang, G., Huang, T.-C., Lin, K.-P., 2009. Red blood cell velocity measurements of complete capillary in finger nail-fold using optical flow estimation. Microvasc. Res. 78, 319–324.
24. Ying, X., Xiu, R., 1994. Dynamic and still microcirculatory image analysis for quantitative microcirculation research. Proc. SPIE 2168, 98-108.

Tables

Table 1. Mean difference and limit of agreement of RBC velocity in Bland-Altman plots.

	CCM vs VI		OFM vs VI	
Conditions	Mean difference (mm/s)	Limits of agreement (mm/s)	Mean difference (mm/s)	Limits of agreement (mm/s)
Normal (n=25)	-0.033	-0.151 to 0.086	-0.040	-0.200 to 0.120
Resting, T_1 (n=16)	0.004	-0.060 to 0.068	-0.012	-0.073 to 0.049
Inflation, T_2 (n=11)	-0.005	-0.028 to 0.019	-0.014	-0.053 to 0.025
Occlusion, T_3 (n=11)	-0.006	-0.028 to 0.016	0.004	-0.006 to 0.014
Release, T_4 (n=12)	-0.054	-0.208 to 0.101	-0.090	-0.500 to 0.310
T_1 to T_4 (n=50)	-0.014	-0.108 to 0.080	-0.030	-0.240 to 0.180
All cases (n=75)	-0.020	-0.124 to 0.083	-0.030	-0.220 to 0.160

Figure captions

Fig. 1.
(a) A plasma gap is traveling down through the venous site as shown in 3 consecutive frames. The movement and velocity (V_{f2f}) can be determined by calculating the Euclidean distance of the red squares between two adjacent frames. (b) Assume that the plasma gap drawn a track (white line) in the space-time diagram. The line's slope represents the RBC velocity over the three frames (V_{std}). The average of V_{f2f} and V_{std} was considered as the reference velocity (V_{ref}).

Fig. 2.
(a) One of the ten vessels from healthy volunteers in resting condition and (b) the vessel's corresponding space-time diagram generated from a 10-second blood flow video. Seven red strips indicated seven data point of averaged RBC velocity.

Fig. 3.
Cuff pressure applied on subjects' wrist which varied the blood flow into four different phases, *i.e.*, T_1: resting (0 mmHg), T_2: inflation (0 to 180 mmHg), T_3: occlusion (180 mmHg), and T_4: release (180 to 0 mmHg).

Fig. 4.
(a) One of the twelve vessels from healthy subjects and the vessel's corresponding space-time diagram generated from the blood flow video of each condition ((b) T_1: resting, (c) T_2: inflation, (d) T_3: occlusion, and (e) T_4: release.

Fig. 5.
Relative errors of cross-correlation and optical flow estimations of RBC velocity in normal condition. Data from 10 vessels in resting condition were all presented. The number of velocity assessment points was 25.

Fig. 6. Relative errors of cross-correlation and optical flow estimations of RBC velocity in four blood flow conditions: (a) T_1: resting, (b) T_2: inflation, (c) T_3: occlusion, and (d) T_4: release.

Fig. 7.
(a) Relative errors of cross-correlation and optical flow estimations of RBC velocity in occlusion-release blood flow conditions (combined data of T_1 to T_4). (b) Relative errors of cross-correlation and optical flow estimations of RBC velocity in normal and variation flow conditions (combined data of all cases).

Fig. 8.
Agreement between (a) the cross-correlation and visual inspection methods and (b) the optical flow and visual inspection methods for RBC velocity estimation for normal cases.

Fig. 9.
Agreement between the cross-correlation and visual inspection methods for RBC velocity measurement in four blood flow conditions: (a) T_1: resting, (b) T_2: inflation, (c) T_3: occlusion, (d) T_4: release and (e) T_1 to T_4.

Fig. 10.
Agreement between the optical flow and visual inspection methods for RBC velocity measurement in four blood flow conditions: (a) T_1: resting, (b) T_2: inflation, (c) T_3: occlusion, (d) T_4: release and (e) T_1 to T_4.

Fig. 11.
Agreement between (a) the cross-correlation and visual inspection methods and (b) the optical flow and visual inspection methods for RBC velocity measurement in normal and various flow conditions (combined data of all cases).

Figure 1

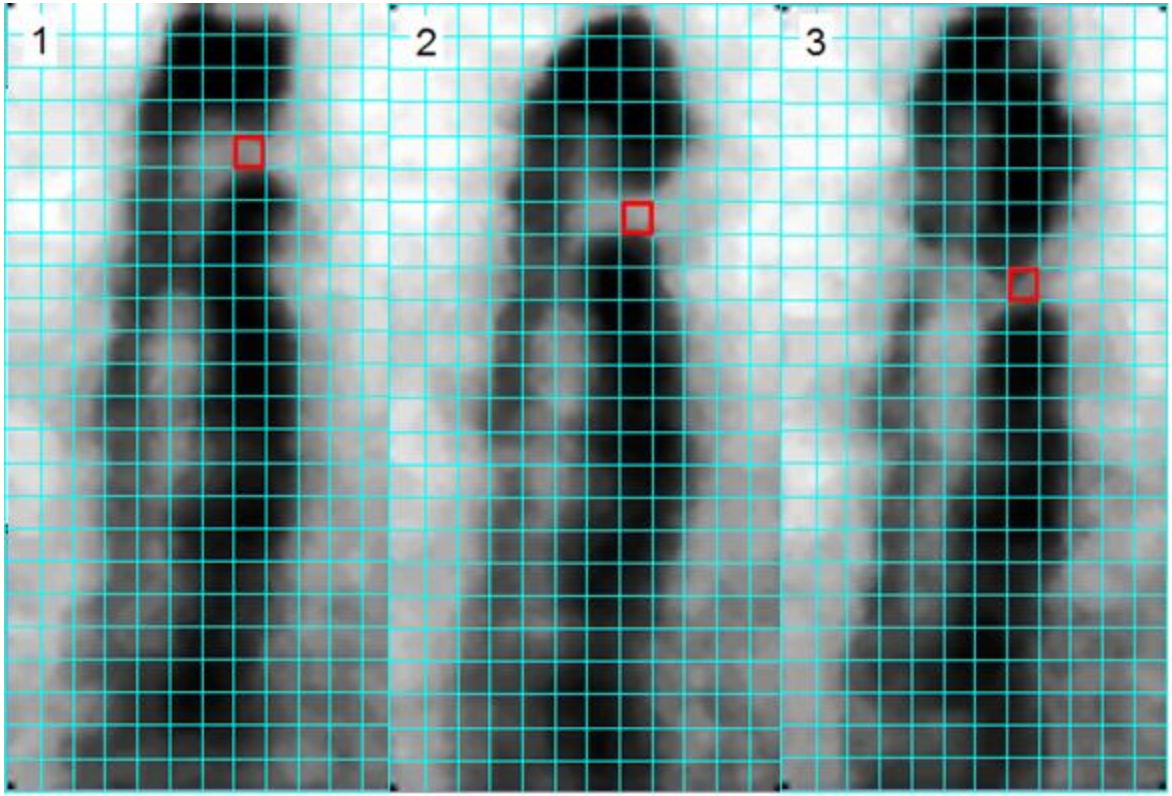

(a)

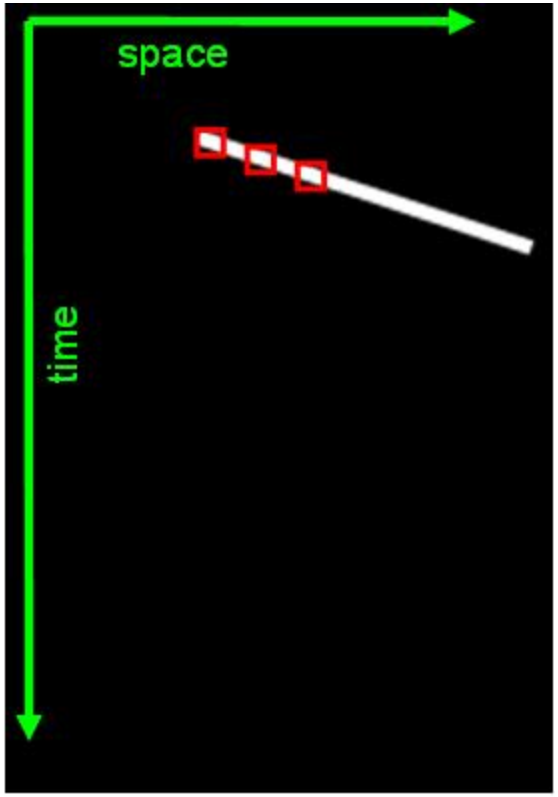

(b)

Figure 2

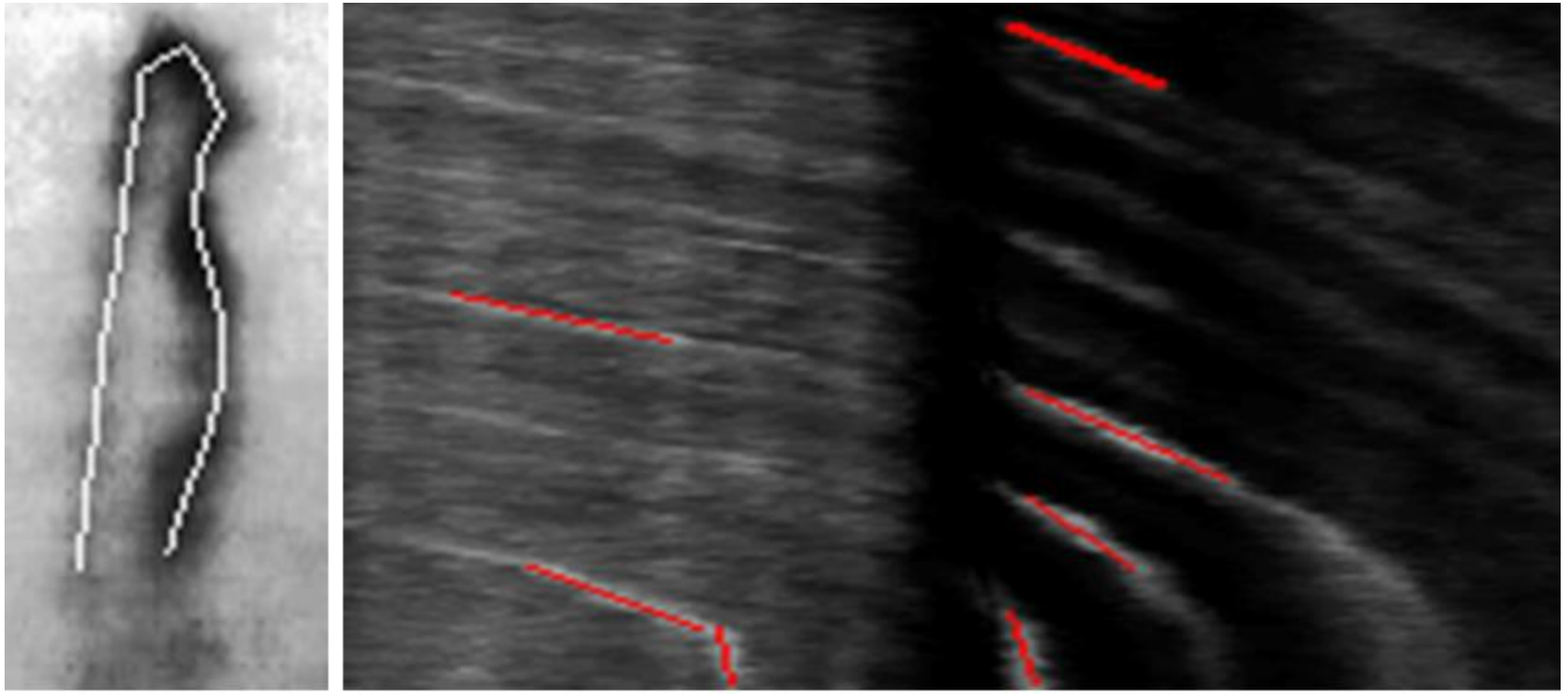

(a) (b)

Figure 3

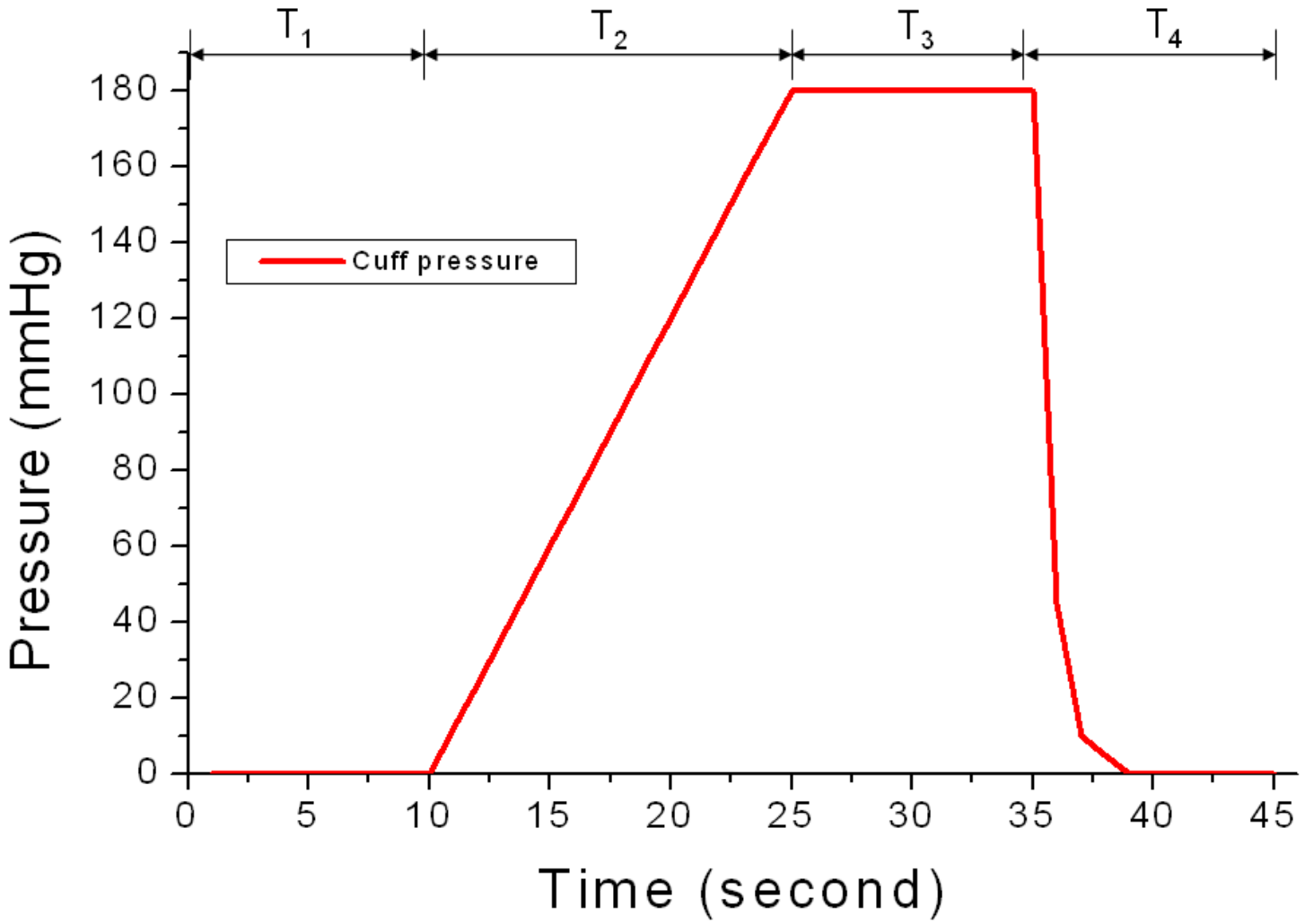
T1
T2
T3
T4
Cuff pressure
Pressure (mmHg)
0
20
40
60
80
100
120
140
160
180
0
5
10
15
20
25
30
35
40
45
Time (second)

Figure 4

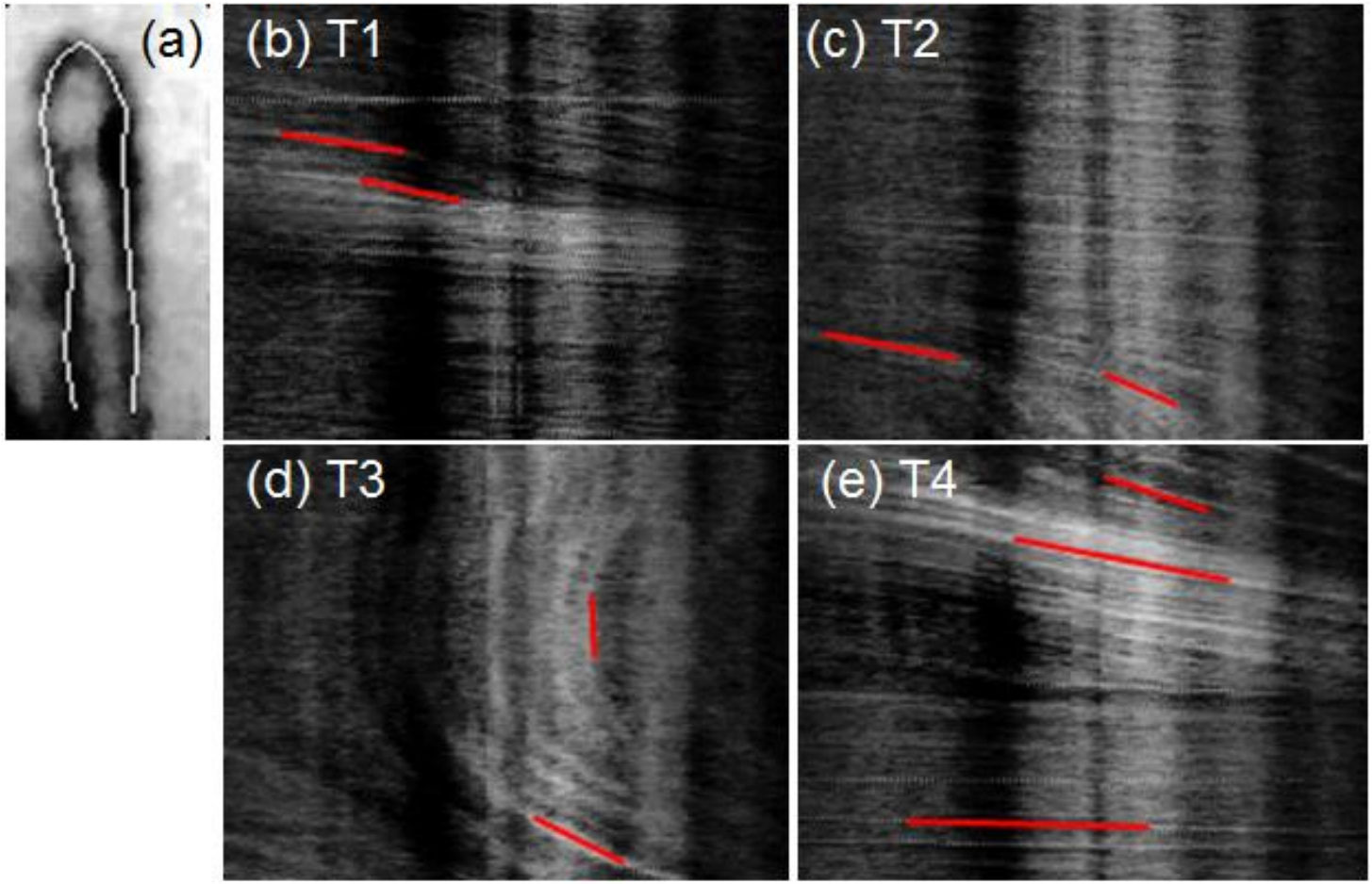

Figure 5

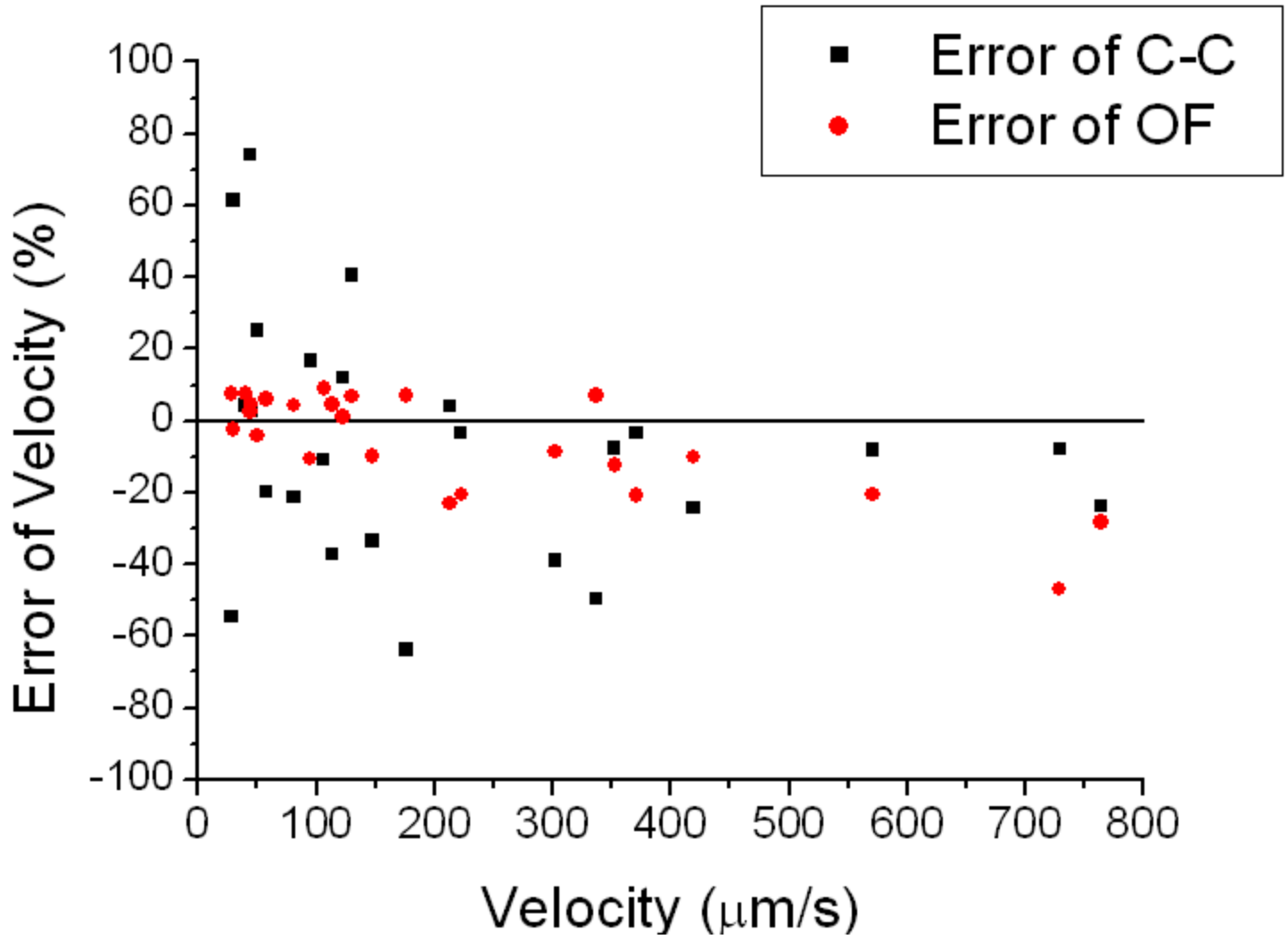
Error of C-C
Error of OF
Error of Velocity (%)
100
80
60
40
20
0
-20
-40
-60
-80
-100
0
100
200
300
400
500
600
700
800
Velocity (μm/s)

Figure 6

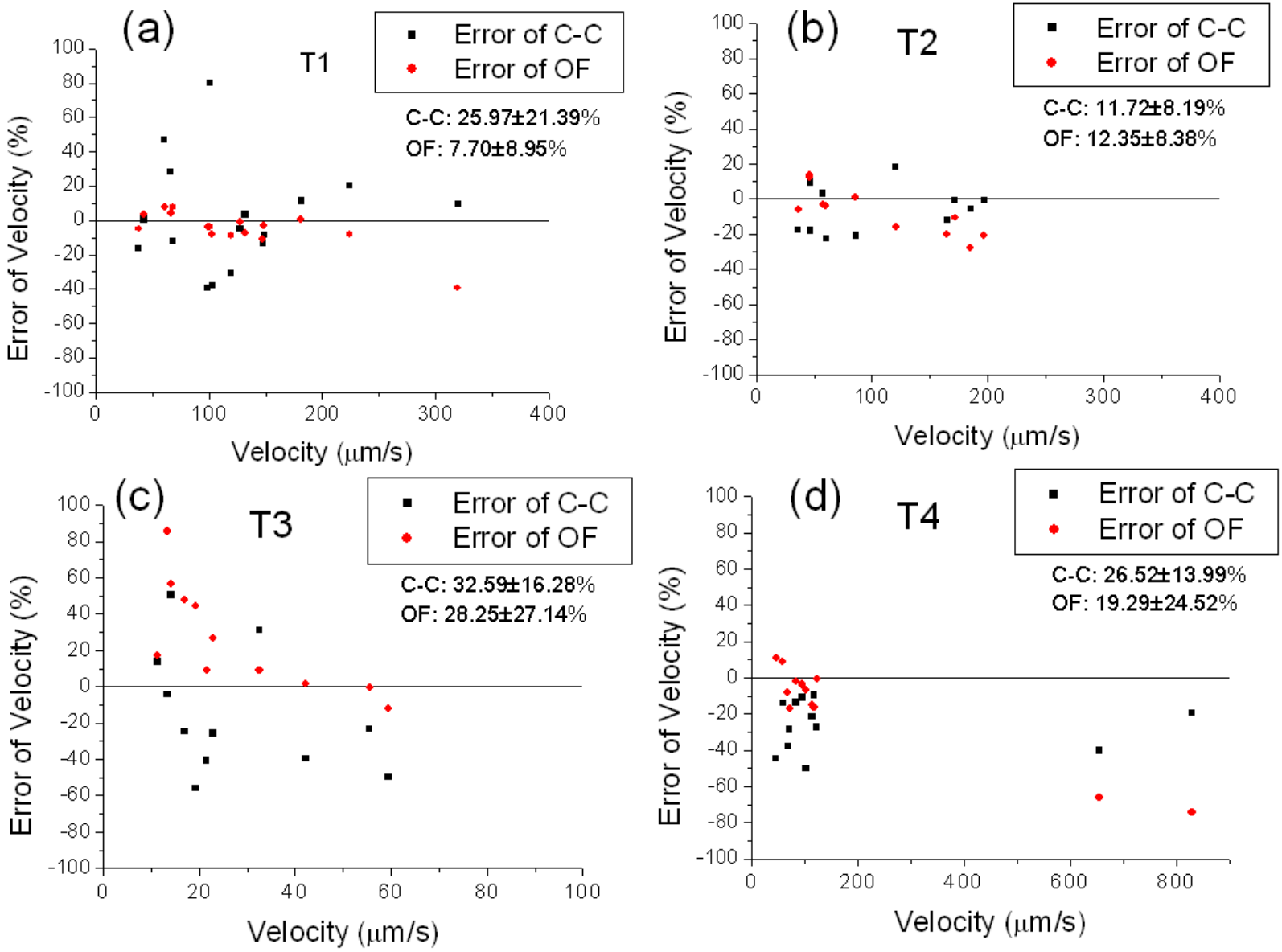
(a)
T1
Error of C-C
Error of OF
C-C: 25.97±21.39%
OF: 7.70±8.95%
Error of Velocity (%)
Velocity (μm/s)
(b)
T2
Error of C-C
Error of OF
C-C: 11.72±8.19%
OF: 12.35±8.38%
Error of Velocity (%)
Velocity (μm/s)
(c)
T3
Error of C-C
Error of OF
C-C: 32.59±16.28%
OF: 28.25±27.14%
Error of Velocity (%)
Velocity (μm/s)
(d)
T4
Error of C-C
Error of OF
C-C: 26.52±13.99%
OF: 19.29±24.52%
Error of Velocity (%)
Velocity (μm/s)

Figure 7

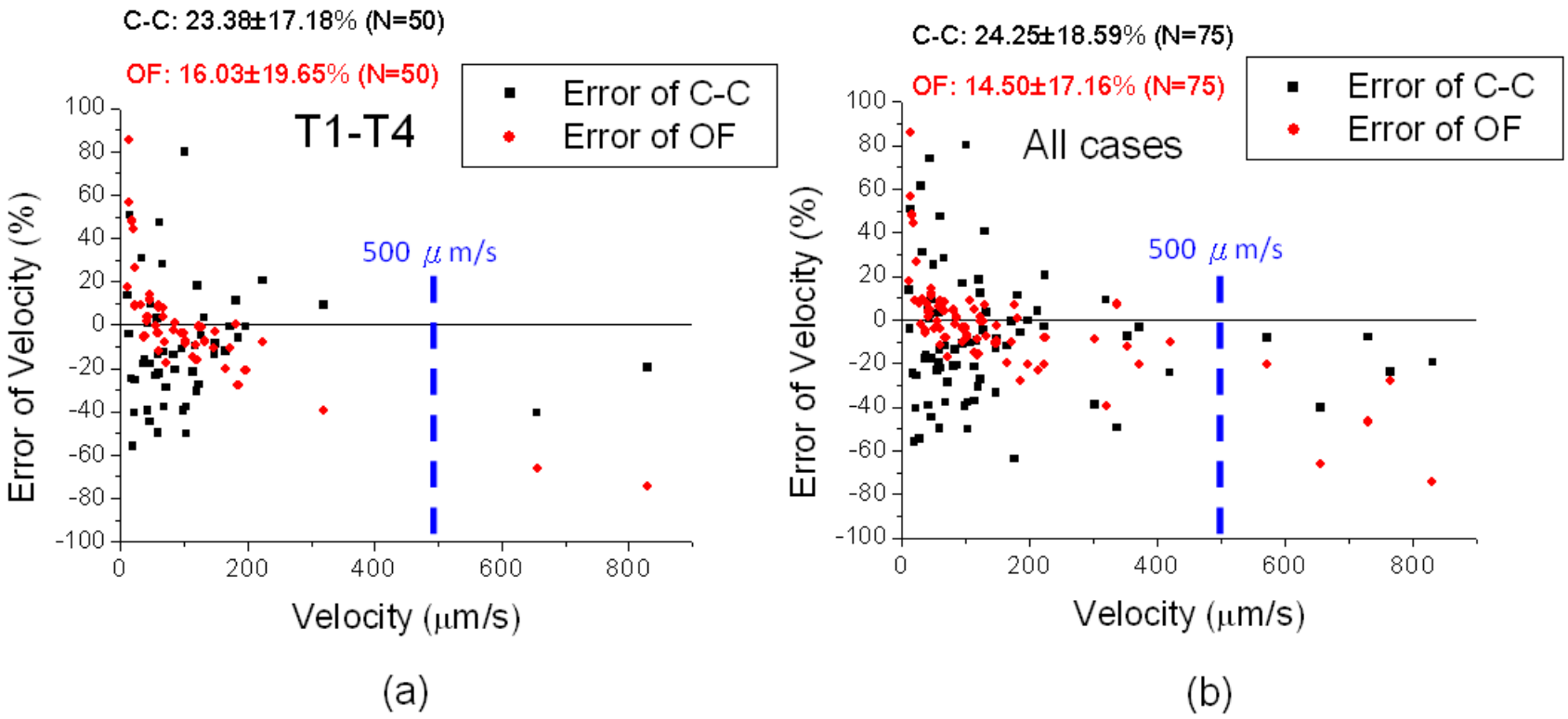
C-C: 23.38±17.18% (N=50)
OF: 16.03±19.65% (N=50)
T1-T4
Error of C-C
Error of OF
500 μm/s
Error of Velocity (%)
Velocity (μm/s)
(a)
C-C: 24.25±18.59% (N=75)
OF: 14.50±17.16% (N=75)
All cases
Error of C-C
Error of OF
500 μm/s
Error of Velocity (%)
Velocity (μm/s)
(b)

Figure 8

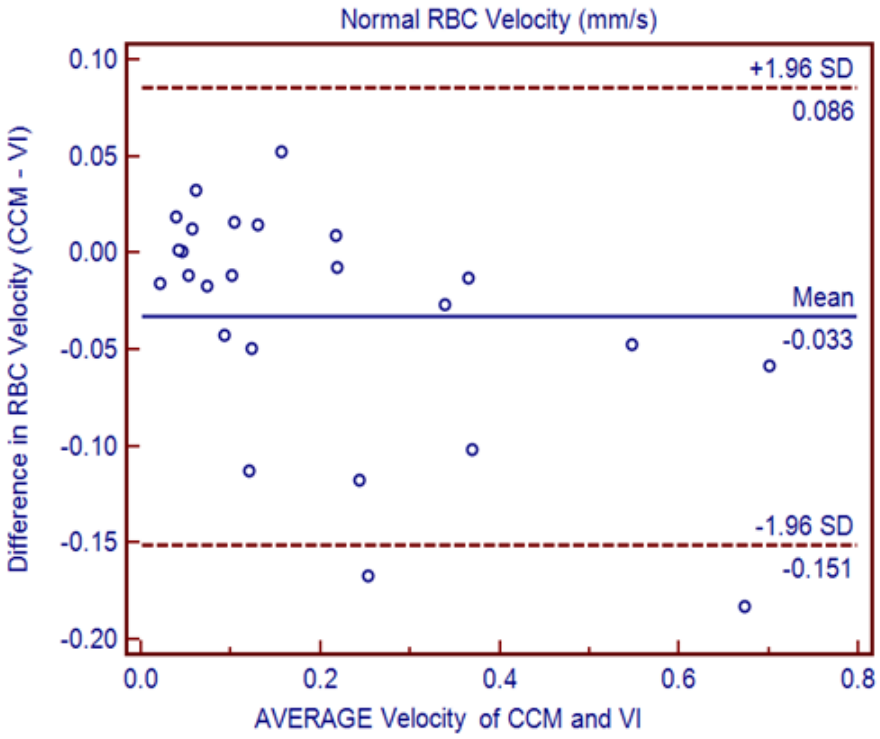
Normal RBC Velocity (mm/s)
+1.96 SD
0.086
Mean
-0.033
-1.96 SD
-0.151
Difference in RBC Velocity (CCM - VI)
AVERAGE Velocity of CCM and VI
0.10
0.05
0.00
-0.05
-0.10
-0.15
-0.20
0.0
0.2
0.4
0.6
0.8

(a)

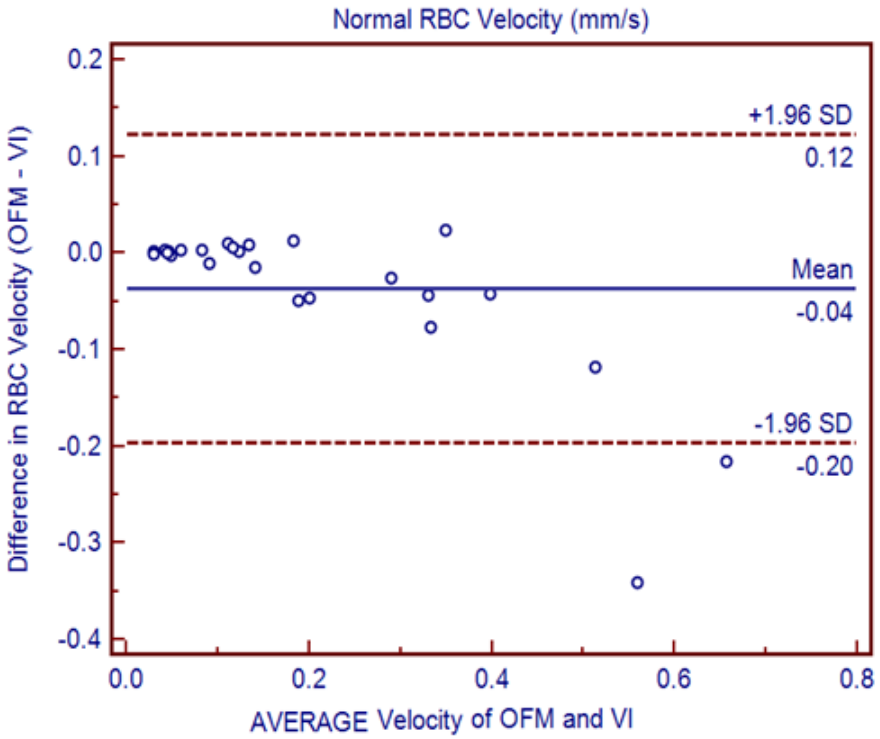
Normal RBC Velocity (mm/s)
+1.96 SD
0.12
Mean
-0.04
-1.96 SD
-0.20
Difference in RBC Velocity (OFM - VI)
AVERAGE Velocity of OFM and VI
0.2
0.1
0.0
-0.1
-0.2
-0.3
-0.4
0.0
0.2
0.4
0.6
0.8

(b)

Figure 9

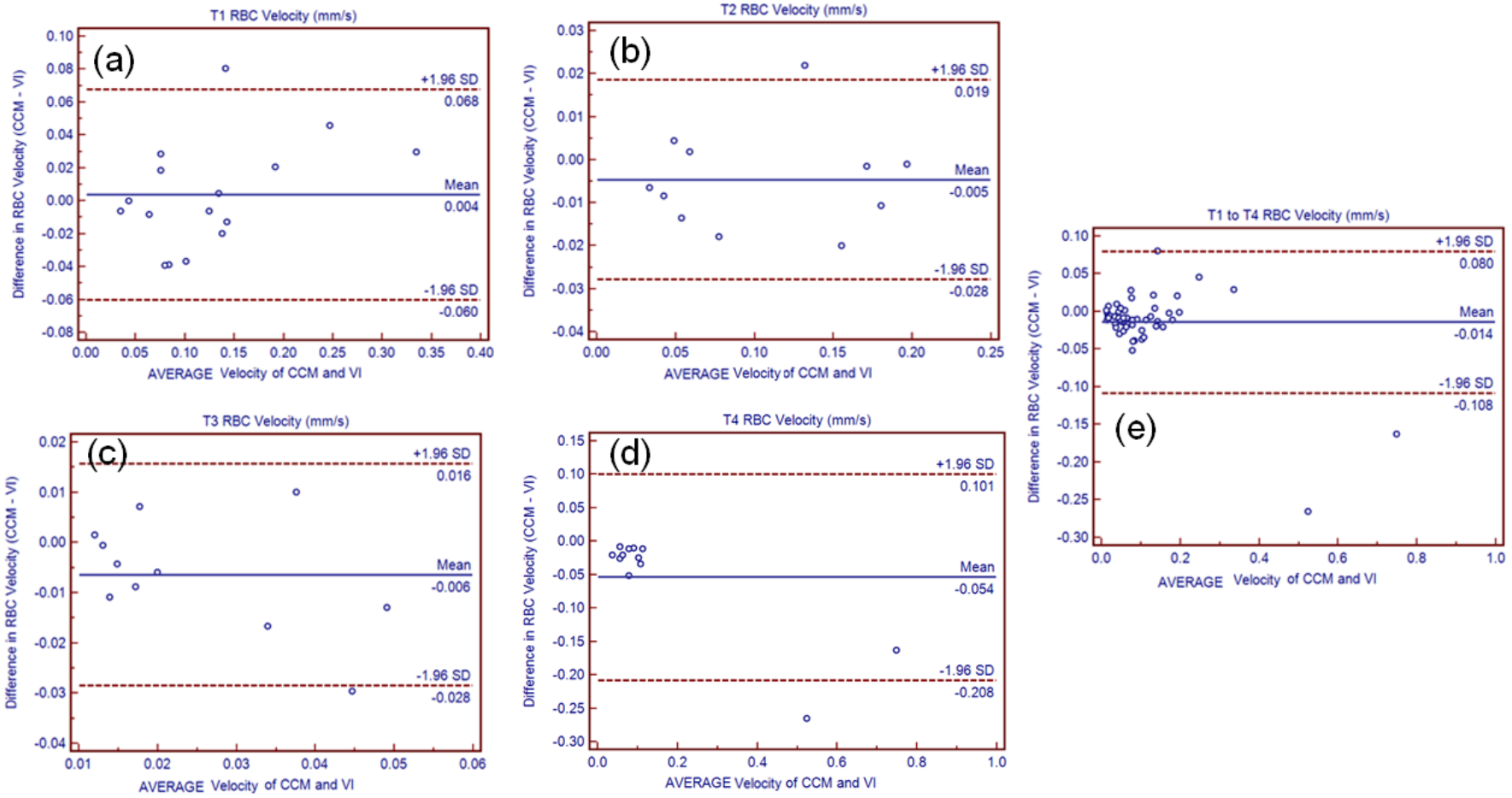
T1 RBC Velocity (mm/s)
(a)
+1.96 SD
0.068
Mean
0.004
-1.96 SD
-0.060
Difference in RBC Velocity (CCM - VI)
AVERAGE Velocity of CCM and VI
T2 RBC Velocity (mm/s)
(b)
+1.96 SD
0.019
Mean
-0.005
-1.96 SD
-0.028
Difference in RBC Velocity (CCM - VI)
AVERAGE Velocity of CCM and VI
T3 RBC Velocity (mm/s)
(c)
+1.96 SD
0.016
Mean
-0.006
-1.96 SD
-0.028
Difference in RBC Velocity (CCM - VI)
AVERAGE Velocity of CCM and VI
T4 RBC Velocity (mm/s)
(d)
+1.96 SD
0.101
Mean
-0.054
-1.96 SD
-0.208
Difference in RBC Velocity (CCM - VI)
AVERAGE Velocity of CCM and VI
T1 to T4 RBC Velocity (mm/s)
(e)
+1.96 SD
0.080
Mean
-0.014
-1.96 SD
-0.108
Difference in RBC Velocity (CCM - VI)
AVERAGE Velocity of CCM and VI

Figure 10

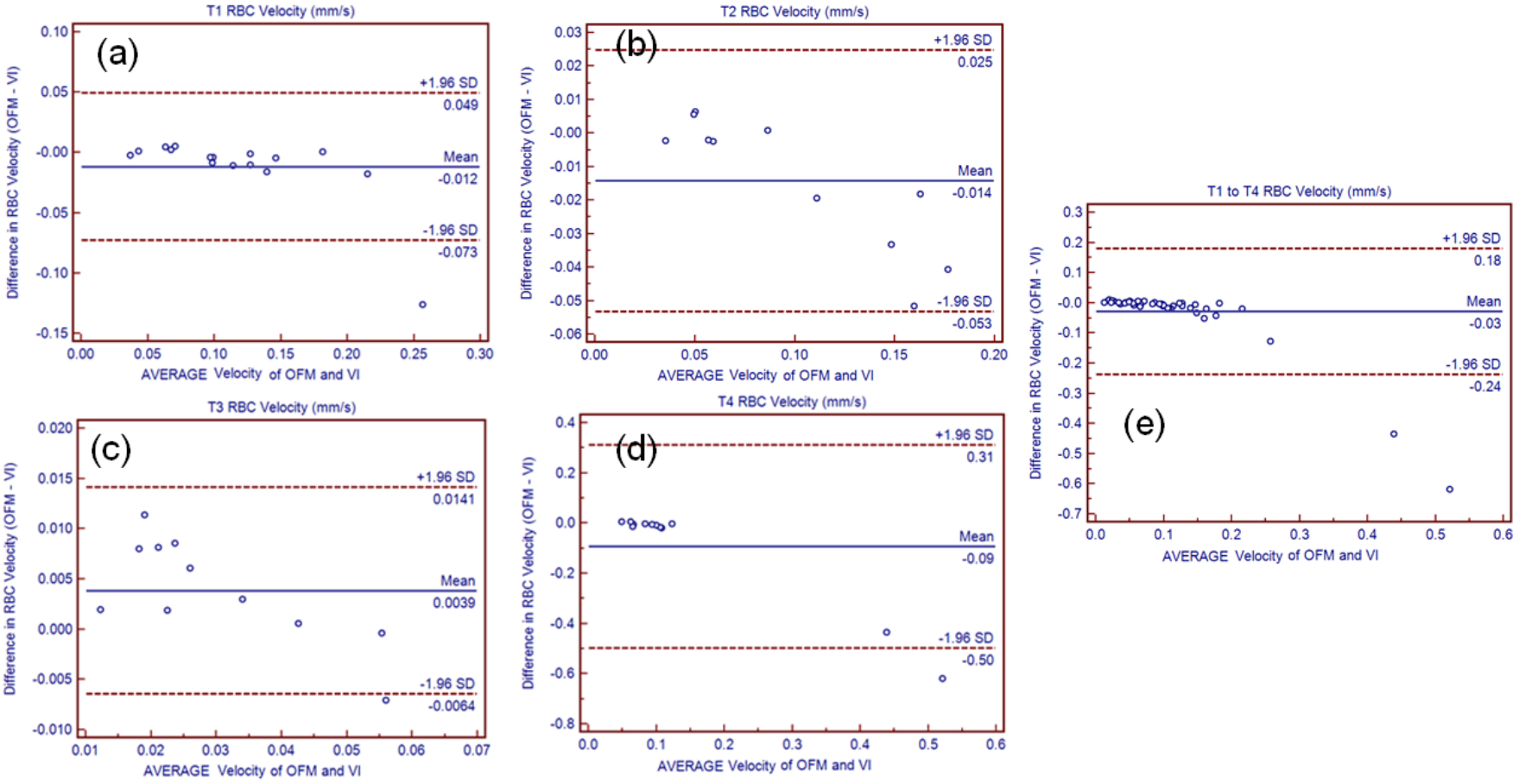
T1 RBC Velocity (mm/s)
(a)
+1.96 SD
0.049
Mean
-0.012
-1.96 SD
-0.073
Difference in RBC Velocity (OFM - VI)
AVERAGE Velocity of OFM and VI
T2 RBC Velocity (mm/s)
(b)
+1.96 SD
0.025
Mean
-0.014
-1.96 SD
-0.053
Difference in RBC Velocity (OFM - VI)
AVERAGE Velocity of OFM and VI
T3 RBC Velocity (mm/s)
(c)
+1.96 SD
0.0141
Mean
0.0039
-1.96 SD
-0.0064
Difference in RBC Velocity (OFM - VI)
AVERAGE Velocity of OFM and VI
T4 RBC Velocity (mm/s)
(d)
+1.96 SD
0.31
Mean
-0.09
-1.96 SD
-0.50
Difference in RBC Velocity (OFM - VI)
AVERAGE Velocity of OFM and VI
T1 to T4 RBC Velocity (mm/s)
(e)
+1.96 SD
0.18
Mean
-0.03
-1.96 SD
-0.24
Difference in RBC Velocity (OFM - VI)
AVERAGE Velocity of OFM and VI

Figure 11

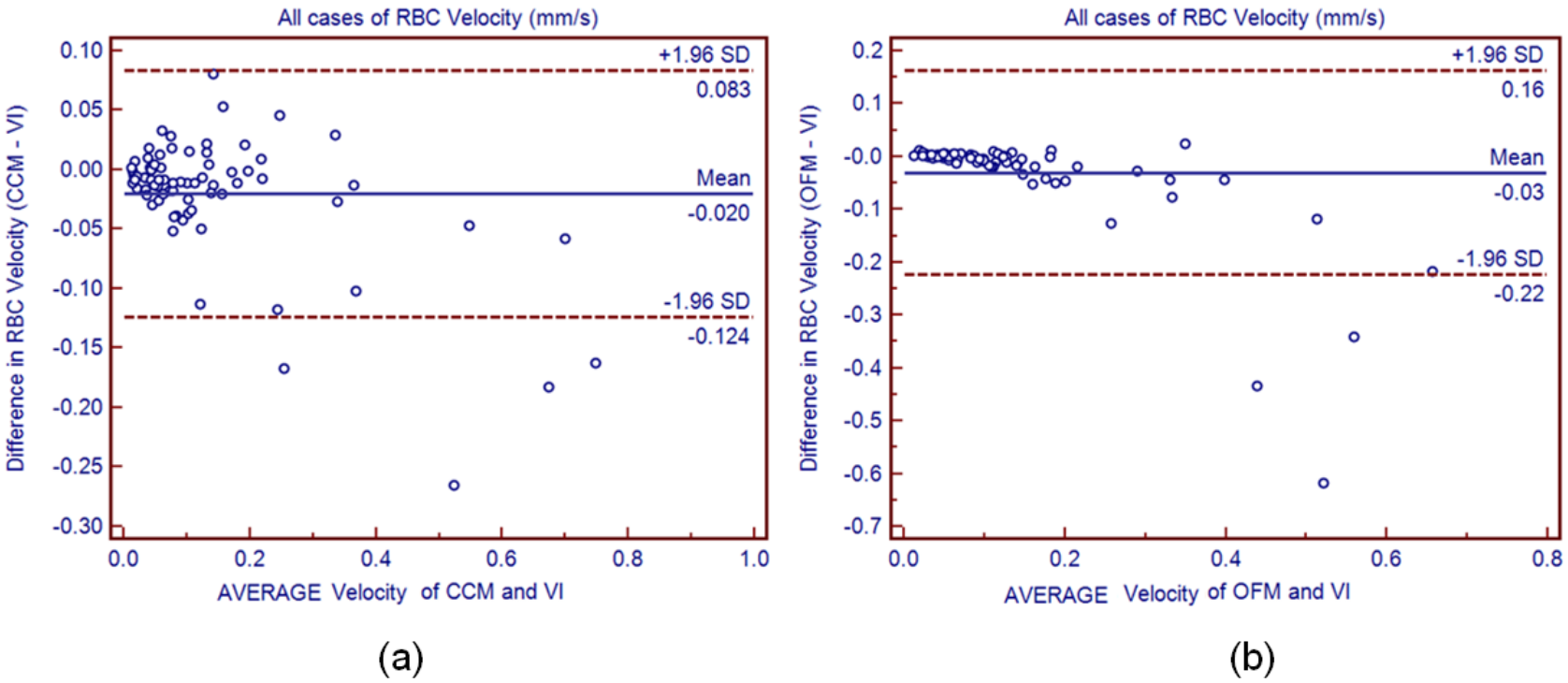
All cases of RBC Velocity (mm/s)
+1.96 SD
0.083
Mean
-0.020
-1.96 SD
-0.124
Difference in RBC Velocity (CCM - VI)
AVERAGE Velocity of CCM and VI
0.10
0.05
0.00
-0.05
-0.10
-0.15
-0.20
-0.25
-0.30
0.0
0.2
0.4
0.6
0.8
1.0
(a)
All cases of RBC Velocity (mm/s)
+1.96 SD
0.16
Mean
-0.03
-1.96 SD
-0.22
Difference in RBC Velocity (OFM - VI)
AVERAGE Velocity of OFM and VI
0.2
0.1
-0.0
-0.1
-0.2
-0.3
-0.4
-0.5
-0.6
-0.7
0.0
0.2
0.4
0.6
0.8
(b)